

On the influence of imaging conditions and algorithms on the quantification of surface topography

U. WENDT*, K. STIEBE-LANGE* & M. SMID†

**Otto-von-Guericke University Magdeburg, School of Materials Science; Universitaetsplatz 2, 39106 Magdeburg, Germany*

†*Carleton University Ottawa, School of Computer Science; 1125 Colonel By Drive, Ottawa, Ontario, Canada K1S 5B6*

Key words. Algorithm, confocal laser scanning microscopy, fractal dimension, surface area, surface topography, topometry.

Summary

The influence of the microscopical magnification resulting in different voxel size and shape and of the algorithm on parameters used for the quantification of the surface topography is studied using topographical images obtained by confocal laser scanning microscopy. Fracture surfaces and wire-eroded surfaces of steel were used as samples. The values obtained for the global topometry parameters normalized surface area, mean profile segment length and fractal dimension depend with different degrees on the microscopic magnification and on the algorithm used to compute these values. The topometry values can only be used to establish correlations between the topography and materials properties and for the modelling of surface generating processes if the imaging and computing details are given.

Introduction

Materials surfaces contain information about the mechanism of the surface generation process and about the factors influencing this mechanism and thereby the surface topography. Those factors are, for example, the crystal structure (including crystal lattice defects and residual stresses), the microstructure of the material, the kind of generation process (e.g. the kind of load in mechanical testing, wear, coating process and cutting process) and the external conditions (temperature, loading speed, chemical environment). Characterization of surfaces, in particular fracture surfaces, is an area of investigation that can provide an understanding of the relationship between the surface topography and the microstructure, the mechanical properties and the other factors mentioned above.

For a long time the aim of researchers has been to extract this information from surface topographies in order to enhance the interpretation and understanding of the material's behaviour.

The quantification of surface topographies is necessary to distinguish surfaces that show no differences by visual inspection, and to establish quantitative correlations with materials properties. Quantification is also necessary to obtain numbers for numerical simulation and modelling of surface topographies, and for comparison of surface qualities.

In recent years, the possibilities for surface topography quantification have been broadened by the availability of new imaging methods, which are able to image surfaces three-dimensionally. Among these methods are confocal laser scanning microscopy (CLSM) (Wilson, 1992), white light interferometry (Schroeder *et al.*, 1999) and scanning force microscopy (SFM) (Schwarz, 1997). The long used stereophotogrammetry using stereo-pairs obtained by scanning electron microscopy (Boyd, 1973) underwent a revitalization due to increased computing power (Scherrer & Kolednik, 2000) and the application of a surface decoration method (Marschall *et al.*, 2000). The reconstruction of 3D-images from optical slices, which are obtained with conventional (non-confocal) optical microscopes, known as extended focus imaging, can be performed with fast software products (Yamaguchi *et al.*, 1999) to yield topographical images.

All these methods produce three-dimensional images with a scaling for all three dimensions, that is the x -, y - and z -axes in the orthogonal coordinate system. In the resulting images, the height of each surface point is encoded as a grey value. This overcomes the three-dimensional characterization of surfaces by two-dimensional height profiles, obtained by sectioning fracture surfaces and drawing the profiles.

The three-dimensional images are used to quantify the topography of very different kinds of surfaces, for example, fracture surfaces and wear surfaces (Anamaly *et al.*, 1995;

Correspondence: U. Wendt. Tel.: + 49 391 671 4542; fax: + 49 391 671 4569; e-mail: ulrich.wendt@mb.uni-magdeburg.de

Ling *et al.*, 1990) and engineering surfaces (Lange *et al.*, 1993; Mainsah *et al.*, 2001).

For quantification of the topographies, several parameters can be used, such as the standardized roughness parameters for machined surfaces (roughness average/ R_a , root mean square roughness/RMS), the ratio of the true and the projected area (normalized surface area R_s ; introduced by Underwood as surface roughness parameter; Underwood, 1991) and the fractal dimension (Kaye, 1994; Russ, 1994). The two-dimensional parameter normalized profile length (profile roughness parameter; Underwood, 1991), which is estimated on height profiles, extracted from three-dimensional images, can also be used.

The fractal dimension is often used as a global topometry parameter (Li *et al.*, 1995; Li *et al.*, 1996), despite the fact that its use for characterizing surfaces is limited (Wendt & Blumenauer, 1999). The fractal dimension is estimated not only on height profiles extracted from three-dimensional images, but also from vertical cuts through fracture surfaces and the application of various methods (Balankin *et al.*, 2000).

One special application concerning the fractal dimension of ductile fractures has been reported (Tanaka *et al.*, 1998, 1999). They apply the box-counting methods to lines which have been manually drawn into SEM images.

Many very useful results were obtained for the interpretation of materials behaviour with the help of the quantitative characterization of surface topographies (Exner, 2001).

A problem arises when topometry values obtained by using different imaging methods, different imaging parameters and different computing algorithms, are compared. The same problem occurs if these values are used for the modelling of surface generating processes, for example, the modelling of fracture paths (Borodich, 1999). The resulting values of the topometry parameters depend on the microscopical magnification, the measuring algorithm, and on the variables used within the measuring algorithms, for example, the mesh size in surface area calculations. Often this fact is not taken into account when topometry values are compared, although it is obvious that the measured values of some topometry parameters depend on the measuring conditions. For example, the true surface area for a given surface increases with optical magnification, because more details of the surface topography are included in the image, as has been shown by the estimation of the normalized surface area based on the profile length obtained from different SEM magnifications of sections perpendicular to fracture surfaces (Li *et al.*, 1995). Another example is that roughness measurements made with different instruments can yield different roughness values because features with different sizes are measured. Very sophisticated mathematical techniques have been proposed for the calculation of different types of fractal dimension (Falconer, 1997), but only little attention has been paid to the practical estimation of the fractal dimension using real objects and to taking into account different measuring conditions.

For the fractal dimension it is emphasized that each of the methods for the measurement of the fractal dimension can deliver a different value (Dubuc *et al.*, 1989; Russ, 1994), but the imaging and specific computing conditions are not taken into account. For example, the value for this parameter received by the slit-island method depends on the yardstick size used to measure the area and the perimeter of the slits and islands (Lung & March, 1999).

The comparison of absolute values of the fractal dimension, obtained from several materials and by different techniques, can hardly contribute to the description and interpretation of material's properties and its mechanical behaviour (Lea Cox & Wang, 1993).

In this paper, results are shown of a systematic investigation of the dependency of the values of some global topometry parameters on the imaging conditions and on the algorithms used to analyse the images.

Our intention is a methodological study, focusing more on the imaging and measuring procedure than on delivering a correlation between the topometry data and the surface generation processes and the relationship between the surface topographies and the material's properties.

Materials and methods

Materials

The surface topography quantification was performed on fracture surfaces of a low-alloyed steel (German brand: 10MnMoNi5-5) (Fig. 1) and on wire eroded surfaces of a stainless steel (German brand: X6CrNiTi 18.11) (Fig. 2).

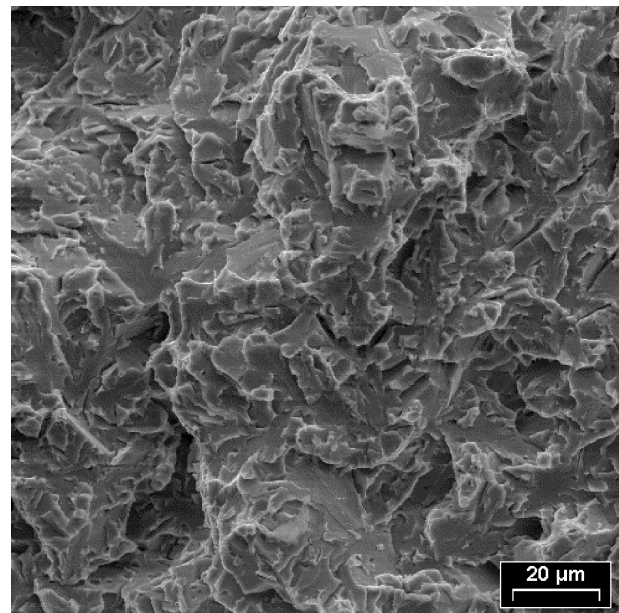


Fig. 1. Fracture surface of the steel 10MnMoNi5-5; impact test at a temperature of $-120\text{ }^{\circ}\text{C}$; SEM image.

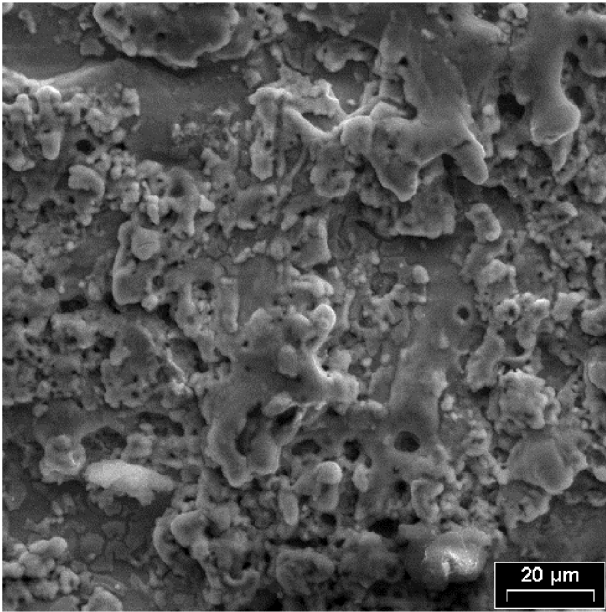


Fig. 2. Eroded surface of the stainless steel X6CrNiTi1 8-11; SEM image.

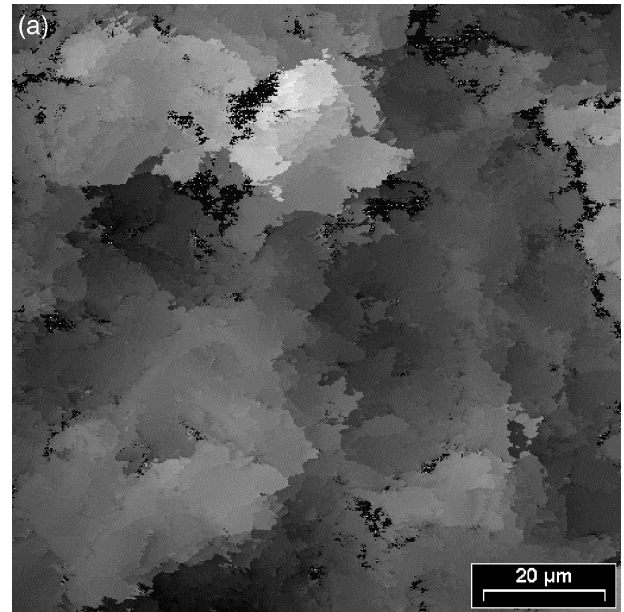
These surfaces were chosen because they have been the subject in other studies, and differences in the topography of specimens obtained at different fracture temperature, or different eroding conditions, respectively, should be known. These differences cannot be seen by visual inspection of SEM images, but can be detected by quantification of the surface topographies. The fracture surfaces were obtained by the Charpy impact test of standard V-notched specimens at low temperature ($-120\text{ }^{\circ}\text{C}$).

The eroded specimen was processed by wire-guided electrical discharge machining at a voltage of 85 V, a current of 160 A with a discharge time of $1.74\text{ }\mu\text{s}$ and an idle time of $20\text{ }\mu\text{s}$.

Method

The surfaces were imaged by confocal laser scanning microscopy (CLSM). With this method, the surface topography is optically sectioned, and a topographical image can be reconstructed from the resulting slice series (Wilson, 1992). The surface topography quantification was done using topographical images, where the height is presented as a grey value or colour code (Figs 3 and 4). The instrument used (TCS 4D/Leica) is a beam scanner with an argon laser. Only reflected light was used for the imaging. All specimens were sputter-coated with gold to produce a homogeneous reflection of the surface. The coating process is necessary, because some parts of the microstructure and therefore of the surface do not reflect light sufficiently.

The imaging conditions are listed in Table 1. An image size of 512×512 pixels was chosen for all images.



(b)

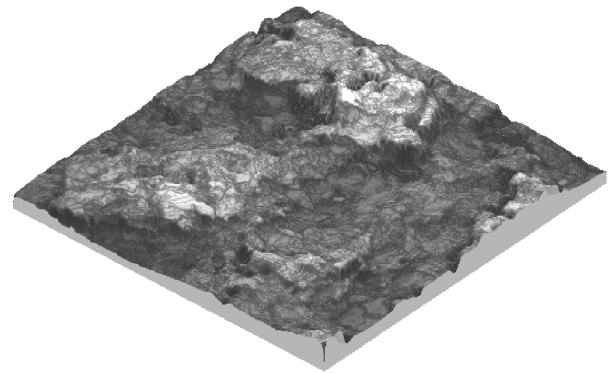


Fig. 3. Topographical image (a) and parallel projection (b) of the fracture surface of the low alloyed steel 10MnMoNi5-5; CLSM image.

The optical resolution is small in some cases, because some microscope objectives possess relatively small numerical apertures. This is because of the necessity of using objectives with a large working distance (sometimes more than 1.5 mm) for the investigation of rough fracture surfaces.

In order to avoid the influence of textures of the topographies, the fractured specimens were always placed in the same direction on the microscope stage with the notch directed to the upright position.

The voxel shape was always cubic except for those images, which were used to study the influence of the voxel shape and size on the values of the topometry parameters. In these cases, the z scaling of the voxels was modified by the variation of the step size of the z -movement of the microscope stage during image capture with the confocal microscope. This means that the total height difference of the surface was divided in different numbers of optical slices.

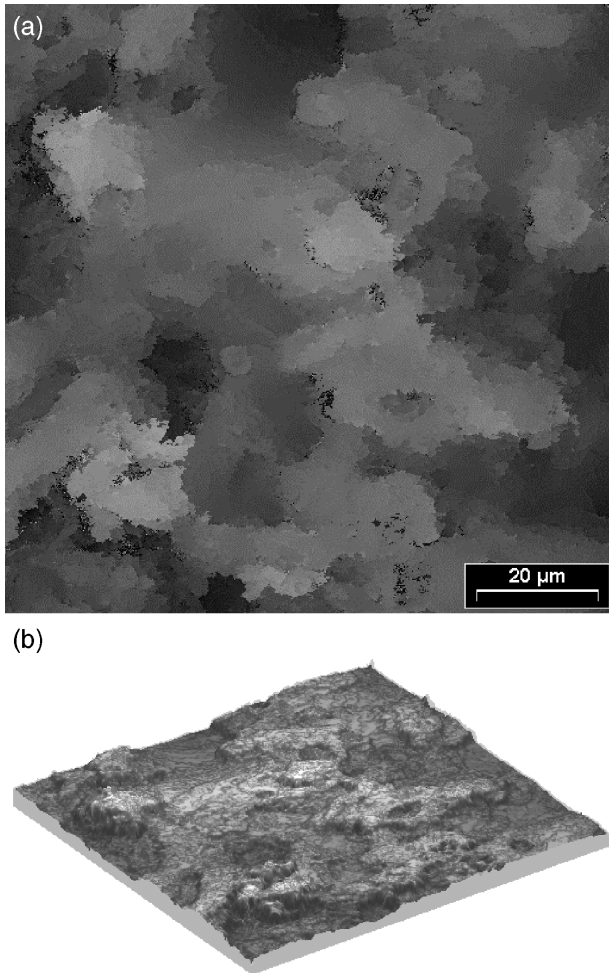


Fig. 4. Topographical image (a) and parallel projection (b) of the eroded surface of the stainless steel X6CrNiTi 18-11; CLSM image.

All image-processing steps were run on an image analysing system (analySIS-pro/SIS GmbH, Münster, Germany). The noise filter and the quantification algorithms were implemented using the interpreter language of this image analyser, which is related to the C++ programming language.

Noise filter

In CLSM images, noise is usually present, due to surface regions for which the normals have small angles to the illuminating laser beam. The intensity of light reflected from those regions back to the objective is too small to give a sufficient signal. The result is single pixels or small groups of pixels in the topographical image, which, by the image reconstruction

algorithm, are set to the lowest (here: zero) or the highest grey value present in the image. In particular, this happens when rugged fracture surfaces are imaged.

To remove these imaging artefacts, a noise filter was applied to all topographical images to correct those single pixels or pixel groups. This noise filter was used because the known mean and median filters, which remove noise pixels as well, also change the grey value of almost all other pixels in the image.

With a 3×3 kernel, the grey values of such pixels are substituted by the mean grey value of the surrounding eight pixels, whereby pixels with the same grey value as the centre pixel, which will be corrected, are not taken into account while calculating the mean value. That way all single pixels as well as groups of two and three pixels with the lowest and highest grey values are corrected. All other pixels are not changed. The quantification was then performed without any further image enhancement.

Quantification parameters

The normalized surface area (R_s), the mean linear profile segment length (PSL) and the fractal dimension (D) were studied as parameters for the quantification of the surface topographies.

Normalized surface area, R_s

The normalized surface area, R_s (Underwood, 1991), is the ratio of the true surface area, A , and the projected area, A_o : $R_s = A/A_o$.

This parameter is sensitive to the area of the surface but not necessarily to the ruggedness. Surfaces with relatively flat but rough hills with small topography features and surfaces with large but smooth planes can result in the same value for the normalized surface area. Therefore, only surfaces with similar topography features should be compared using R_s .

The true surface area was obtained by triangulating the image in the following way. Each pixel is regarded as a point whose x - and y -coordinates are those of the centre of the pixel and whose z -coordinate is equal to the grey value of the pixel. We used a grid size, a_{tri} , in the range 1 to 7. For any such value, a_{tri} , we covered the image using squares consisting of $(a_{tri} + 1) \times (a_{tri} + 1)$ pixels. Examples are given in Fig. 5(a) (where $a_{tri} = 1$) and Fig. 5(b) (where $a_{tri} = 3$). For each square with corners p , q , r and s (these are the three-dimensional points corresponding to the four pixel corners), we computed the areas of the four three-dimensional triangles $a = (p,q,r)$,

Table 1. CLSM parameters for imaging the surfaces.

Objective magnification/numerical aperture	5×/0.12	10×/0.25	20×/0.45	40×/0.6	100×/0.75
Scan area ($\mu\text{m} \times \mu\text{m}$)	2000 × 2000	1000 × 1000	500 × 500	250 × 250	100 × 100
Side length of cubic voxel (μm)	3.91	1.95	0.98	0.49	0.195

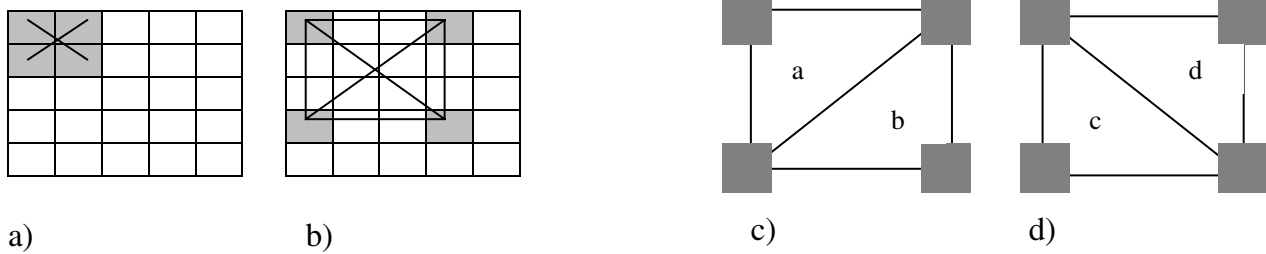


Fig. 5. Measuring size [grid size $a_{tri} = 1$ (a) and grid size $a_{tri} = 3$ (b)] and geometry (c) and (d) for the estimation of the true surface area by triangulation.

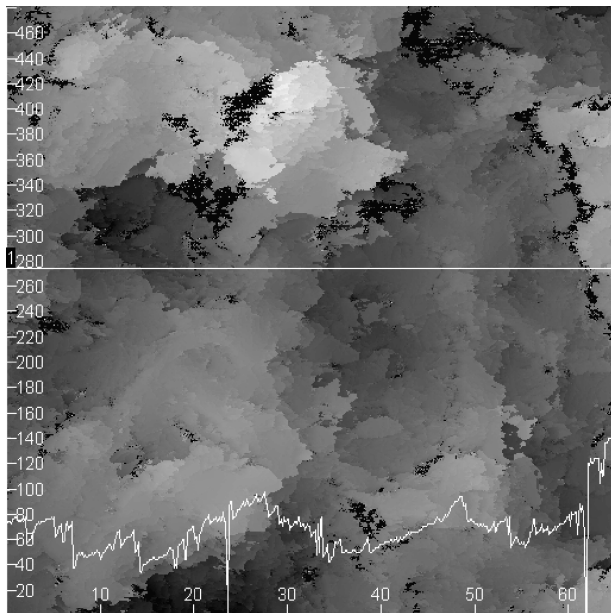


Fig. 6. CLSM image of a low-alloyed steel fracture surface with an extracted height profile as used for the estimation of the PSL.

$b = (p,r,s)$, $c = (p,q,s)$ and $d = (q,r,s)$. For example, the area a is equal to 0.5 times the length of the vector $(q - p) \times (r - p)$. (This vector is the cross product of the two vectors $q - p$ and $r - p$). The true area of this square was obtained as $(a + b + c + d)/2$, see Fig. 5(c) and (d).

Mean profile segment length

For the estimation of the profile segment length (PSL), height profiles were extracted from the topographical image (Fig. 6) and the mean values of the linear segments contained in these profiles were calculated.

The Euclidean distance between the endpoints of a linear segment was measured as the segment length. A line between two adjacent pixels is also regarded as a linear segment. The segment length was not estimated using profiles drawn in an image and an image analyser to measure the length of segments. In this case, the problem of how to draw a line connecting two pixels in adjacent rows as solved by the Bresenham algorithm (Bresenham, 1965) is avoided.

For each image, 20 profiles parallel to the x - and to the y -axes were used for the estimation of the mean value. In no case, were differences detected between the mean PSL values of the 10 profiles parallel to x , and the 10 profiles parallel to y .

PSL was chosen as a parameter because it is correlated to the size of planar regions in fracture surface topographies, e.g. the size of fracture facets in brittle fracture surfaces, which are related to the crack path. The aim was to investigate the dependency of the PSL values on the voxel size and shape.

Fractal dimension

More than a dozen methods are known for the estimation of the fractal dimension. We chose the slit-island method and the two-dimensional box-counting method, because both methods are based on relatively simple algorithms and work properly on all investigated specimens. The methods are well known (Mandelbrot, 1977; Kaye, 1994; Russ, 1994; Bunde & Havlin, 1995) and their mathematical backgrounds do not need to be described here in detail, but the measuring procedures and the calculating algorithms will be outlined, because they can influence the quantification results. It is necessary to know details of the estimation of the fractal dimension if values reported by different authors are compared. For the other topometry parameters, a log-log plot was drawn and values were calculated from the slope of the curve, which we call fractal dimension, as well, because these parameters depend on an imaging or calculation ruler. As no discussion of the usefulness of the application of the fractal dimension as topometry parameter has been given here, no attention is paid to the question of whether the investigated fracture and erode surfaces are self-similar or self-affined, and how far this can influence the values received for the fractal dimension.

Slit-island method

In the topographical images, height slices are performed with different grey value thresholds, leading to islands and lakes in the image (Fig. 7). The area and the perimeter of these islands and lakes were measured (Mandelbrot, 1977; Lung & March, 1999). The grey value thresholds were set at 20, 30, 50, 60 and 80% of the maximum grey value present in the image. Islands and lakes touching the image border are not taken into account.

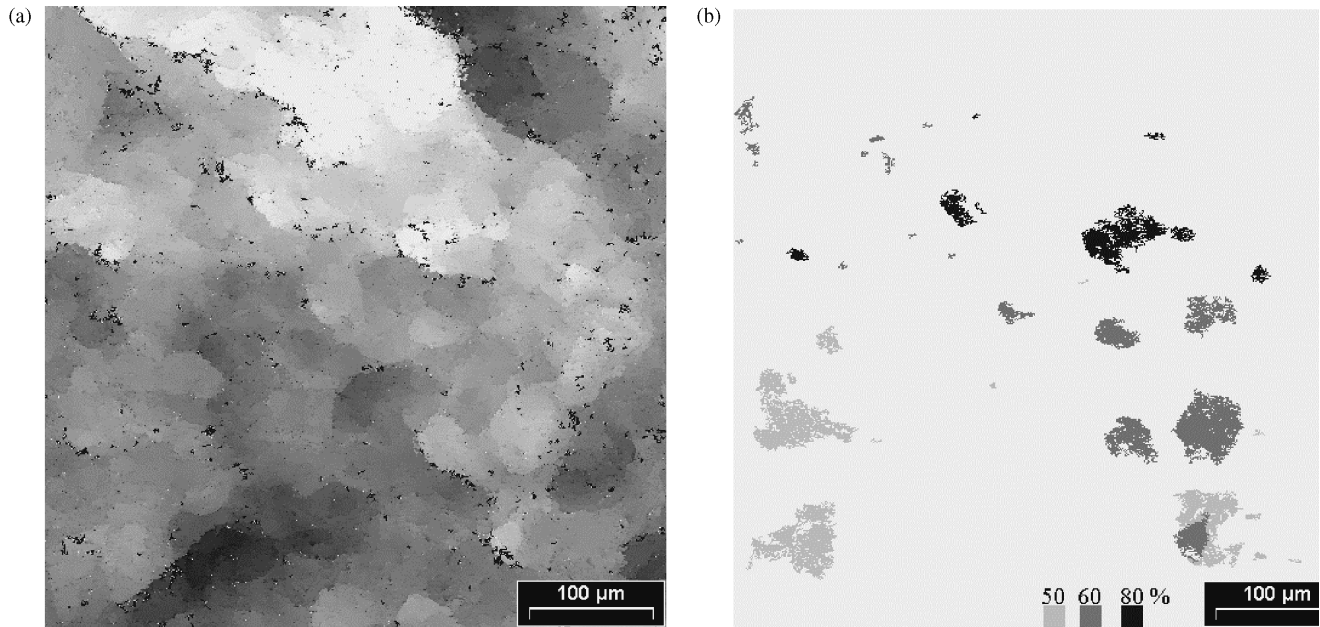


Fig. 7. Principle of the slit-island method; topographical CLSM image of a fracture surface (a) and the resulting image after slicing at 80, 60 and 50% of the maximum grey value (b).

The area and the perimeter of all objects are measured and a log–log plot is drawn. The fractal dimension is calculated from the slope of the curve $D_{si} = 2/\text{slope}$.

2D-box-counting method

From the topographical image, height profiles were extracted and drawn as x - y curves, which were masked with grids of different grid (box) sizes (Bunde & Havlin, 1995). The number of hits (boxes covering at least one pixel) is counted and a log–log diagram is drawn for box size vs. number of hits. The box-counting fractal dimension is calculated from the slope of the resulting curve by $D_{2dbox} = \text{slope}$.

The box sizes were 4, 5, 6, 8, 10, 12, 16 and 20 pixels. These sizes are applicable to a measuring field of 480×480 pixels. With other box sizes, images with 512×512 pixels are not completely covered. The measuring algorithm was implemented as a kernel. The often applied and faster method of using an image operation with masks of different mesh sizes leads to an overlay of the grid line and the profile. Pixels lying on the grid lines are not counted. From each topographical image, 10 height profiles were extracted parallel to both the x - and y -axes.

Results

Influence of the image orientation on the topometry values

It can be assumed that for certain surfaces the topometry values depend on the orientation of the specimens with regard to the measuring direction. This is possible with fracture surfaces or with wear surfaces, if some of the topography features are

orientated in a preferred direction. Using profiles extracted from the images at different orientations with respect to the crack direction, the quantification of fracture surface topographies was proposed (Gokhale & Underwood, 1990; Li *et al.*, 2001).

The PSL and the 2d-box-counting fractal dimension were estimated on height profiles, which were extracted from topographical images. For the specimens investigated here, no differences could be detected for profiles, extracted parallel to the x -axis and parallel to the y -axis as well as for profiles extracted in both 45° directions. Therefore, it can be concluded that the investigated surfaces show no preferred orientation of the topography features.

Measurement of PSL using images with different voxel sizes

The measurement of the PSL, using images that are obtained with different magnifications and therefore different cubic voxel sizes in the topographical image, was performed to show the dependency of the PSL values on the voxel size. This relationship has to be taken into account if the PSL values are used for the numerical modelling of crack paths.

Figure 8 shows the dependency of the PSL value on the voxel size; the slope indicates a significant dependency of the PSL values on the voxel size, as proposed. From the slope of the curve, a kind of fractal dimension $D_{PSL} = 1 + \text{slope}$ for profiles can be calculated, which has a value of $D_{PSL} = 1.48$.

Measurement of PSL using images with different voxel shapes

The same region of the surface was imaged with different numbers of optical slices. Thus, voxels result, which have a

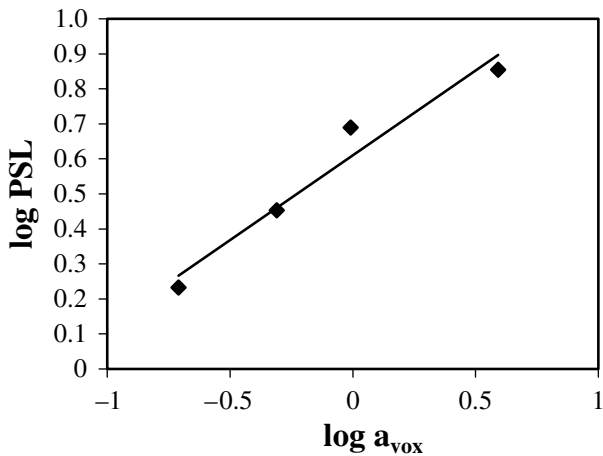


Fig. 8. Dependency of the PSL on the voxel size a_{vox} ; eroded surface of the stainless steel.

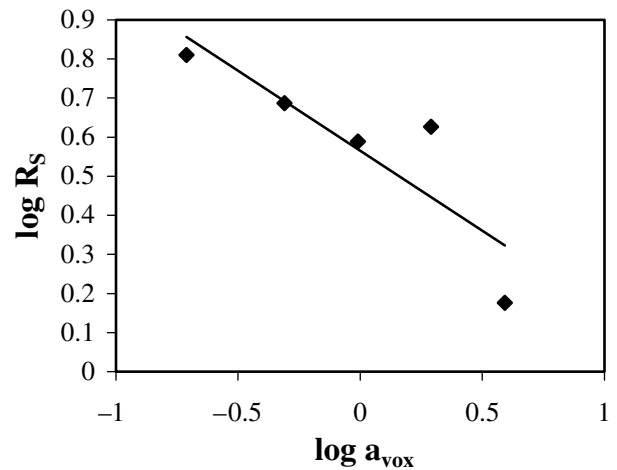


Fig. 10. Log–log plot of normalized surface area R_s vs. size of the cubic voxels a_{vox} ; wire-eroded surface of the stainless steel.

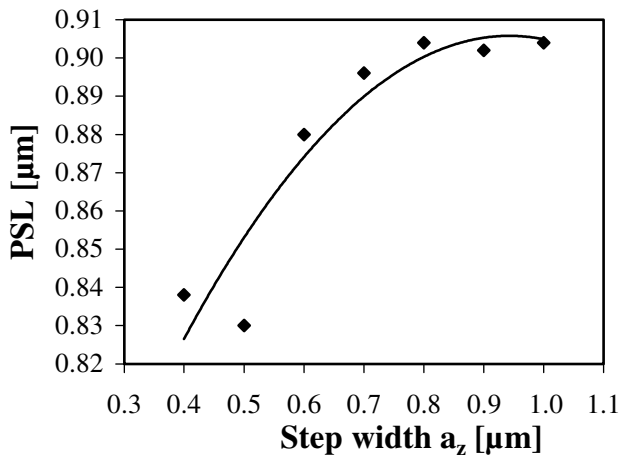


Fig. 9. Relationship between the voxel shape (variation of the z -dimension of the voxels) and the PSL; eroded surface of the stainless steel; x,y -scaling = 0.2 μm , objective 100 \times /0.75.

cubic or a tetrahedral shape and different z -scaling. All other microscope settings were not changed. The influence of the voxel shape on the PSL is demonstrated in Fig. 9.

At first, the PSL increases with growing step width. Then, at a step width of about 0.8 μm , the PSL value becomes constant, so that it can be assumed that a correlation to the axial resolution of 0.77 μm for the used objective exists. Therefore, we draw the conclusion that with step width values greater than the axial resolution, the influence of the voxel's z -dimension on the measured value disappears.

Measurement of R_s using images with different (cubic) voxel size

The triangulation was performed with a fixed triangle size of 1. The influence of the voxel size on the surface area values was investigated using images from different optical magnifications. The z -step width was chosen so that the voxels were cubic.

The log–log plot of the R_s values vs. the voxel size gives an almost straight line for the eroded surface (Fig. 10). From the slope of the curve, the fractal dimension is $D_{R_s \text{ vs } a_{\text{vox}}} = 2 - \text{slope} = 2.41$. A similar result was obtained for the fracture surface.

This method of estimating the fractal dimension is equivalent to methods in which the length of profile lines is measured with different yardstick lengths (ruler or divider method). The simple explanation for the curve in Fig. 10 is that with different voxel sizes topographical features with different sizes are included in the image. With higher magnification, more of the fine details of the topography contribute to the measured surface area. This is only true with voxel sizes greater than or equal to the optical resolution.

Measurement of R_s using different triangle size

The basis of this method is the measurement of the true surface area by triangulation and the calculation of the normalized surface area, R_s (for the algorithm see above). The true surface area was measured with different triangle sizes, a_{tri} . This method is comparable to the divider or yardstick method applied to height profiles (Underwood, 1991; Cox & Wang, 1993) and to a method using different voxel sizes as described earlier. The advantage over the yardstick method is that the measurement is performed using the whole topography and not only height profiles, which are extracted from the topographical images, or from cuts perpendicular to the surface.

The normalized surface area, as expected, depends on the triangulation grid size (Fig. 11 a). From the slopes of the linear curves, a fractal dimension is calculated as D_{tri} with values between 2.54 and 2.70. These values are only true for the given voxel sizes and depend on the voxel size, as shown in Fig. 11 (b).

The combination of the curves in Fig. 11(a) and (b) shows that a bimodal dependency of the R_s values on the imaging conditions and on the computing algorithm exists.

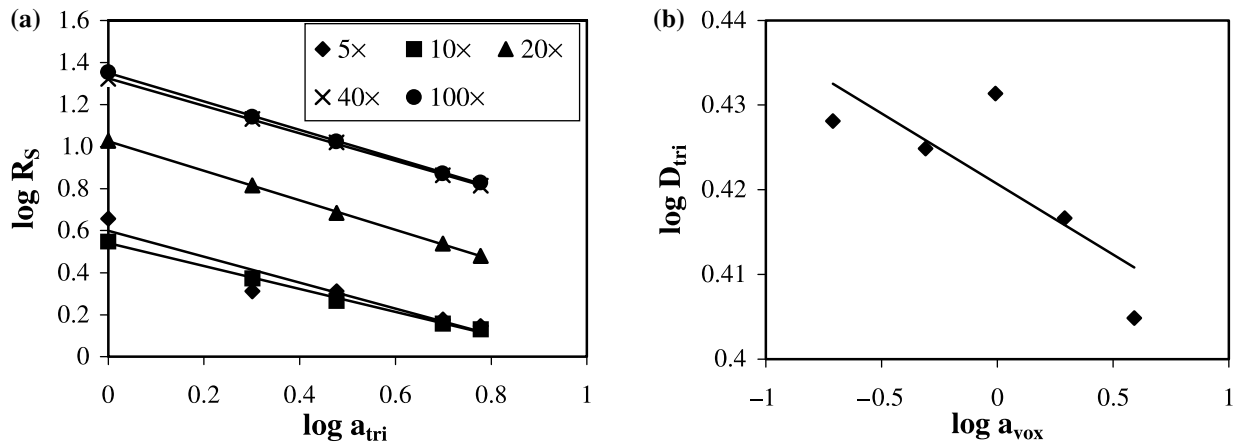


Fig. 11. Log–log plot of normalized surface area R_s vs. size of the measuring grid a_{tri} for the triangulation; fracture surface of the low alloyed steel; cubic voxel sizes (magnification of the used objectives is given) (a) and log–log plot of D_{tri} vs. size of the voxel a_{vox} ; fracture surface of the low alloyed steel (b).

Similar measurements on fracture surfaces based on the height information generated by photogrammetry of stereo pairs obtained by scanning electron microscopy showed that the surface area depends only a little on the triangle size (called point density) (Friel & Pande, 1993).

Fractal dimension measurement using images with different voxel size

The fractal dimension was estimated by the box-counting and by the slit-island method. For the box-counting method, height profiles were extracted from topographical images. The log–log plots of the reciprocal number of hits ($1/N$) vs. the box size (e_{box}) result in nearly straight lines for images with the same voxel size; different curves are obtained for different voxel sizes.

Box-counting was performed for the fracture surface of the low-alloyed steel and for the eroded surface of the stainless steel. In both cases, similar results were noticed.

The values for the fractal dimension D_{2dbox} , directly calculated from the slope of the curves $1/N$ vs. e_{box} as $D_{2dbox} = \text{slope}$, for both materials depend on the voxel size as shown in Fig. 12.

The slit-island method for the estimation of the fractal dimension was performed by slicing the topography at several grey levels. Using the fracture surface of the low-alloyed steel and the eroded surface of the stainless steel as examples, it can be shown that for grey value thresholds at 20, 50 and 80% of the maximal grey value in the image, the log–log plots of the area vs. the perimeter of the lakes result in separate curves for every grey threshold (Fig. 13). In addition, the curves for the lakes and the islands are different.

As shown for the box-counting method, the values of the fractal dimension, obtained by the slit-island method, calculated as $D_{si} = 2/\text{slope}$, depend on the voxel size of the topographical images (Fig. 14).

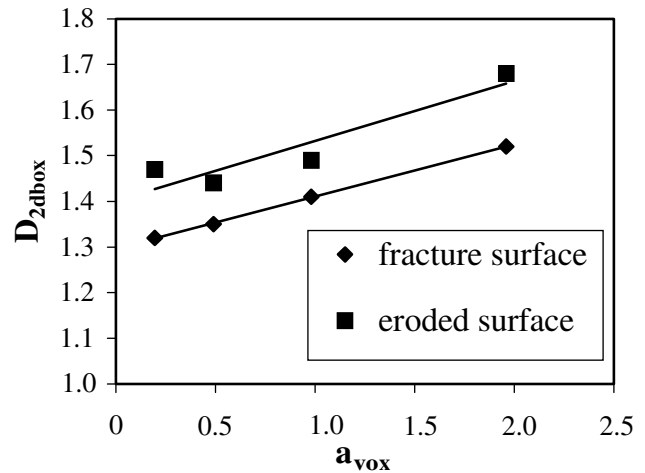


Fig. 12. Relationship between the fractal dimension received by box-counting and the voxel size; fracture surface of the low-alloyed steel and eroded surface of the stainless steel.

These results suggest that by using the slit-island method for the estimation of the fractal dimension it has to be taken into account that the value of the fractal dimension obtained by this method depends not only on the imaging conditions but also on the measuring parameters. The value is influenced by the slicing height and by the selection of whether the lakes or the islands are used for the area-perimeter plot. Additionally, the influence of the voxel size depends on the kind of surface, as could be shown here for a fracture and an eroded surface.

Conclusions

The influence of imaging conditions and computing algorithms on the values obtained by the quantification of surface topographies was studied. As examples, three topometry

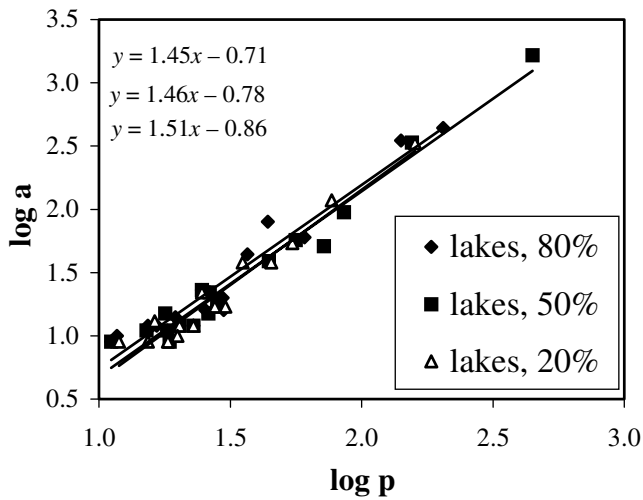


Fig. 13. Slit-island method for the estimation of the fractal dimension; fracture surface of the low-alloyed steel for thresholds at 20, 50 and 80% of grey max (lakes).

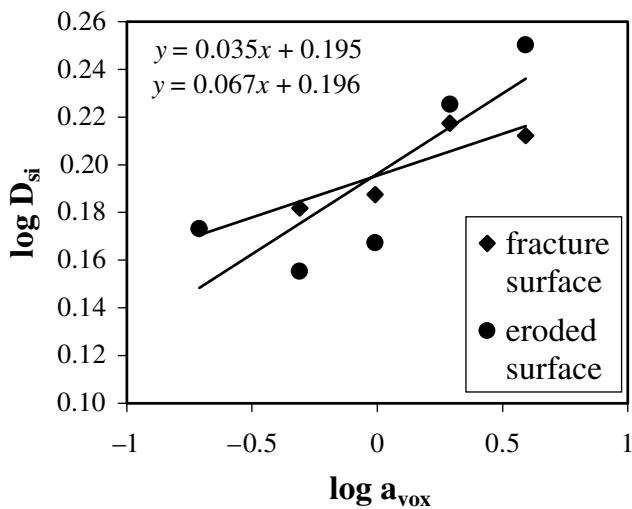


Fig. 14. Dependency of the fractal dimension received by the slit-island method on the voxel size; fracture surface of the low-alloyed steel and eroded surface of the stainless steel.

parameters were chosen: normalized surface area R_s , mean linear profile segment length PSL and fractal dimension D . The surface quantification was performed on topographical images obtained by confocal laser scanning microscopy of fracture surfaces of a low-alloyed steel and of wire-eroded surfaces of a stainless steel.

The CLSM images of these surfaces had to be treated with an image filter to remove noise, which is due to imaging artefacts. A selective image filter was developed in order to correct single noise pixels or small clusters of up to three pixels. Other image filtering operations, for example a mean or median filter,

would lead to the change of almost every pixel and to a loss of information. Therefore, they have to be avoided.

The influence of the imaging conditions (microscopical magnification, thickness of optical slices) on the quantitative results was studied by varying the shape and the size of the voxels in the topographical images.

The dependency of the topometry parameters on the size of cubic voxels is almost linear in log–log plots and can be expressed as a kind of fractal dimension, which is calculated from the slope of the curves. The shape of the voxels expressed as the ratio of the x - and z -scalings (respectively as z -scaling only) has an analogous influence on the topometry parameters. The slope of the resulting log–log plots is different from the curves obtained for the correlation between the voxel size and the topometry parameters. Therefore, using cubic voxels, different values for the fractal dimension result.

The comparison of the fractal dimension values received by the slit-island and the box-counting method, respectively, confirms the results of other authors (Russ, 1994) that different methods can lead to different values of the fractal dimension. Because the experimental results described above show that the dependency of the fractal dimension values on the imaging and calculating conditions are different for both tested methods, it is possible that different correlations of the topometry values with materials properties can result.

Therefore, in equations describing the relation of mechanical parameters, for example the fracture toughness (Mecholsky & Freiman, 1991), to the topometry parameters, the values for coefficients or exponents are only true for a certain set of experimental measuring conditions.

The computing algorithms also have a significant influence on the topometry values. For the estimation of the true surface area by triangulation, a linear dependency on the triangle size results, if a log–log plot is drawn. From the slope of the resulting curve, a value for the fractal dimension is calculated. This method is comparable to the ruler method for the estimation of the fractal dimension applied to height profiles.

However, this value of the fractal dimension itself depends on the voxel size of the images. This is also true for the values of the fractal dimension, which are obtained by the slit-island method. Using the slit-island method for the estimation of the fractal dimension, only one image is necessary, whereas for the estimation of the fractal dimension by calculating the true surface area for different voxel sizes some images are necessary. However, the value for the fractal dimension, obtained by the slit-island method, is only true for the applied size and shape of the voxel. Furthermore, the value depends on the slicing height and on whether the lakes or the islands are used.

The results discussed above are also demonstrated for the mean profile segment length.

As a consequence of the given results, the values of topometry parameters reported by different authors and listed (Milman *et al.*, 1994) can only be compared if they are obtained by identical imaging conditions and identical computing algorithms.

A detailed description of those parameters has to be given with the quantification results. This is particularly necessary for variables such as microscopic magnification, voxel size and shape, applied image filtering procedures to remove noise, and details of the computing algorithm. In any case, the quantification method for a given parameter has to be outlined in detail, for example, the method for estimating the fractal dimension.

The differences between the measured values of the topometry parameters, due to the mentioned influences, can be significant, as demonstrated by the given results. This leads to the question, which value of a topometry parameter should be used for modelling surface generation processes, for instance crack growth and crack paths (Borodich, 1999), and for the calculation of energy balances of those processes.

This question cannot be answered without further study of the dependency of the topometry values on the imaging conditions and on the computing algorithms.

The results described here are of basic interest. It has been shown that topometry values depend on some conditions. Therefore, for the comparison of topometry results and for practical/technical applications of surface topometry, it has to be proved that measurements were performed under identical conditions. This leads to the question of standard specimens. These have to be designed for the various imaging methods, certain magnification ranges, and for different kinds of topography. The latter is necessary, because the influence of imaging conditions differs for the various topographies and for the topography features to be measured, for example roughness, true surface area, and geometric dimensions of single geometric objects, such as planes or dimples.

Similarly, in AFM measurements, the tip geometry influences the topometry results and has to be registered, for instance by a deconvolution routine (Schiffmann *et al.*, 1997).

On the condition that these influences are taken into account, the quantification of surface topographies of all kinds of materials can deliver very useful information for the development of new materials, the understanding of the material's properties and for quality assurance.

Acknowledgement

The authors thank the Deutsche Forschungsgemeinschaft for financial support (projects WE 2301/3-1 and SM 57/4-1).

References

- Anamaly, R.V., Kirk, T.B. & Panzere, D. (1995) Numerical descriptors for the analysis of wear surfaces using laser scanning confocal microscopy. *Wear*, **181**–**183**, 771–776.
- Balankin, A., Morales, D., Gomez Manzilla, J.C., Susarrey, O., Campos, I., Sandoval, F., Bravo, A., Garcia, A. & Galicia, M. (2000) Fractal properties of fracture surfaces in steel. *Intern. J. Fract.* **106**, L21–L26.
- Borodich, F.M. (1999) Fractals and fractal scaling in fracture mechanics. *Intern. J. Fract.* **95**, 239–259.
- Boyde, A. (1973) Quantitative photogrammetric analysis and qualitative stereoscopic analysis of SEM images. *J. Microsc.* **98**, 452–471.
- Bresenham, J.E. (1965) Algorithm for computer control of a digital plotter. *IBM Systems J.* **4**, 25–30.
- Bunde, A. & Havlin, S. (1995) *Fractals in Science*. Springer-Verlag, Berlin.
- Cox, B.L. & Wang, J.S.Y. (1993) Fractal surfaces: measurement and applications in the earth sciences. *Fractals*, **1**, 87–115.
- Dubuc, B., Quiniou, J.F., Roques-Carmes, C., Tricot, C. & Zucker, S.W. (1989) Evaluating the fractal dimension of profiles. *Phys. Rev. A*, **39**, 1500–1512.
- Exner, H.E. (2001) Quantitative metallography in three dimensions. *Prakt. Metallogr.* **38**, 370–384.
- Falconer, K. (1997) *Techniques in Fractal Geometry*. John Wiley, Chichester.
- Friel, J.J. & Pande, C.S. (1993) A direct determination of fractal dimension of fracture surfaces using scanning electron microscopy and stereoscopy. *J. Mater. Res.* **8**, 100–104.
- Gokhale, A.M. & Underwood, E.E. (1990) General method for estimation of fracture surface roughness. Part I. Theoretical aspects. *Metall. Trans.* **A21**, 1193–1200.
- Kaye, B.M. (1994) *A Random Walk Through Fractal Dimensions*. VCM-Verlagsgesellschaft, Weinheim.
- Lange, D.A., Jennings, H.M. & Shah, S.P. (1993) Analysis of surface roughness using confocal microscopy. *J. Mater. Sci.* **28**, 3879–3884.
- Li, X.W., Tian, J.F., Han, N.L. & Wang, Z.G. (1996) Quantitative study of correlation between fracture surface roughness and fatigue properties of SiC/Al composites. *Mater. Lett.* **29**, 235–240.
- Li, X.W., Tian, J.F., Kang, Y. & Wang, Z.G. (1995) Quantitative analysis of fracture surface by roughness and fractal method. *Script. Metall. Mater.* **5**, 803–809.
- Li, X.W., Tian, J.F., Li, S.X. & Wang, Z.G. (2001) Application of a Fractal method to quantitatively describe some typical fracture surfaces. *Mater. Trans.* **42**, 128–131.
- Ling, F.F. (1990) Fractals, engineering surfaces and tribology. *Wear*, **136**, 141–154.
- Lung, C.W. & March, N.H. (1999) *Mechanical Properties of Metals*. World Scientific, Singapore, p. 141.
- Mainsah, E., Greenwood, J.A. & Chetwynd, D.G. (2001) *Metrology and Properties of Engineering Surfaces*. Kluwer Academic Publishers, Boston.
- Mandelbrot, B.B. (1977) *The Fractal Geometry of Nature*. E.H. Freeman and Co, New York.
- Marschall, H.U., Danzer, R. & Pippan, R. (2000) Three-dimensional analysis of decorated ceramic fracture surfaces by automatic stereophotogrammetry. *J. Am. Ceram. Soc.* **83**, 223–225.
- Mecholsky, J.J. & Freiman, S.W. (1991) Relationship between fractal geometry and fractography. *J. Am. Ceram. Soc.* **74**, 3136–3138.
- Milman, V.Y., Stelmashenko, N.A. & Blumenfeld, R. (1994) Fracture surfaces: a critical review of fractal studies and a novel morphological analysis of scanning tunneling microscopy measurements. *Progr. Mater. Sci.* **38**, 425–474.
- Russ, J.C. (1994) *Fractal Surfaces*. Plenum Press, New York.
- Scherrer, S. & Kolednik, O. (2000) A new system for automatic surface analysis in SEM. *Europ. Microsc. Anal.* **00**, 15–17.
- Schiffmann, K., Fryda, M., Goerigk, G., Lauer, R. & Hinze, P. (1997) Correction of STM Tip convolution effects in particle size and distance determination of metal-C:H films. *Fresen. J. Anal. Chem.* **358**, 341–344.
- Schroeder, J.L., Shell, E.B., Matikas, T.E. & Eylon, D. (1999) Development of methods to observe fatigue damage through surface characteristics. *SPIE Conference on Nondestructive Evaluation of Aging Materials and Composites*, 3585, Paper No. 15, March 3.

- Schwarz, U.D. (1997) Scanning force microscopy. *Handbook of Microscopy*, Vol. II (ed. by S. Amelinckx, D. van Dyck, J. van Landuyt and G. van Tendeloo), p. 827. VCH-Verlagsgesellschaft, Weinheim.
- Tanaka, M., Kayama, A., Kato, R. & Ito, Y. (1999) Estimation of the fractal dimension of fracture surface patterns by box-counting method. *Fractals*, **3**, 335–340.
- Tanaka, M., Kayama, A., Sato, Y. & Ito, Y. (1998) Fractal nature of creep-fracture patterns in pure Zn polycrystals. *J. Mater. Sci. Lett.* **17**, 1715–1717.
- Underwood, E.E. (1991) Directed measurement and heterogeneous structures in quantitative fractography. *Acta Stereol.* **10**, 149–165.
- Wendt, U. & Blumenauer, H. (1999) Konfokale Laserrastermikroskopie – Mehr Informationen aus Bruchflächen gewinnen. *Materialprüfung*, **41**, 190–193.
- Wilson, T. (1992) *Confocal Microscopy*. Academic Press, London.
- Yamaguchi, Y., Weldon, M.K. & Morris, M.D. (1999) Fractal characterization of SERS-active electrodes using extended focus reflectance microscopy. *Appl. Spectrosc.* **53**, 127–132.